

Anomalous magnetic viscosity in the bulk-amorphous ferromagnet $\text{Nd}_{60}\text{Fe}_{20}\text{Co}_{10}\text{Al}_{10}$

S. J. Collocott* and J. B. Dunlop

CSIRO Telecommunications and Industrial Physics, Lindfield, 2070, Australia

(Received 13 August 2002; published 27 December 2002)

Magnetic viscosity in ferromagnetic materials is the time dependence of magnetization, $M(t)$, in a constant field and is a result of the thermal activation of irreversible processes. On the major hysteresis loop and over short times, $M(t)$ can be represented by a simple logarithmic monotonic function. The anomalous magnetic aftereffect is the nonmonotonic time dependence of the magnetization. The magnetic viscosity of bulk-amorphous $\text{Nd}_{60}\text{Fe}_{20}\text{Co}_{10}\text{Al}_{10}$ has been studied on the major hysteresis loop and insight into the magnetization processes has been gained from the determination of the magnetic viscosity parameter S , the (rationalized) irreversible magnetic susceptibility χ_{irr} , and fluctuation field H_f . Further measurements on both the lower and upper branches of minor loops or recoil curves, for periods extending to 30 h, were made to investigate any anomalous behavior. On the lower branch of a recoil curve, for certain magnetic prehistories, nonmonotonic behavior is observed, with the magnetization initially increasing, reaching a peak, before decreasing. The Preisach model is used to interpret this nonmonotonic behavior and the relationship between the time taken for the magnetization to reach a peak and the applied magnetic field.

DOI: 10.1103/PhysRevB.66.224420

PACS number(s): 75.60.Lr

I. INTRODUCTION

In a broad physical sense hysteresis can be viewed as having its origin in a system that has a complicated free energy landscape, with many local minima corresponding to metastable states.¹ These metastable states in a ferromagnetic material can be associated with features such as domain walls. Ferromagnetic materials display a time dependence of the magnetization which is known as the magnetic viscosity or fluctuation aftereffect.² Two independent physical descriptions have been developed to describe it, one by Street and Woolley,³ where thermally activated rate processes are considered, involving metastable states with a distribution of activation energies, and the other by Néel (see Ref. 2), where the mechanism is due to random fluctuations of spontaneous magnetization vectors in terms of a fluctuation field. Both predict a logarithmic time dependence for the magnetization. Time-dependent magnetization may also arise from a diffusion mechanism, for example, due to the diffusion of impurity atoms or holes in a ferromagnetic lattice, such as carbon atoms in α -Fe, and displays a temperature dependence typical of diffusion processes.^{2,4}

The time-dependent magnetization $M(t)$ is measured, most commonly, on the major hysteresis loop as a single-step process and is shown diagrammatically in Fig. 1. Initially a magnetic field H_s is applied in the forward direction to achieve saturation of the magnetization of the material. The field is then reduced, reversed on moving to the second or third quadrant, and then held constant at H_1 . Over a limited range of times $M(t)$ can then be described by

$$M(t) = M_0 + S \ln(t + t_0), \quad (1)$$

where S is the magnetic viscosity parameter, M_0 a fitting parameter, and t_0 a fitting parameter to establish a reference time. S in the second and third quadrants is negative and attains its maximum value near the intrinsic coercivity. The ratio of S/χ_{irr} , where χ_{irr} is the irreversible magnetic susceptibility, is defined as the fluctuation field H_f or in the more general form

$$H_f = \frac{S(H, t)}{\chi_{irr}(H, t)} \quad (2)$$

showing that H_f may be time dependent.^{5,6} A two-step process may also be used in a magnetic viscosity experiment; that is, in addition to the single-step process, the magnetic field is paused at H_1 before being increased, moving to a point H_2 on a recoil curve where it is held constant, and $M(t)$ measured. In the two-step experiment, depending on the magnetic prehistory, nonmonotonic behavior of $M(t)$ may be observed. There is the special case in the two-step magnetic viscosity experiment, where a recoil curve is chosen, such that when the applied field is zero, i.e., $H_2 = 0$, the magnetization is zero (see Fig. 1). This is known as dc demagnetization. At zero applied field, relaxation will proceed and the magnetization will begin to increase as the material remagnetizes in a process known as spontaneous remagnetization.

There has been success at modeling both one- and two-step magnetic viscosity experiments with the Preisach model,^{1,7} in which the magnetization is the sum of contributions from a collection of square-loop hysterons, each hys-

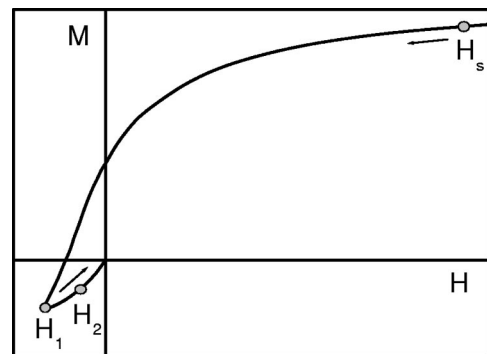


FIG. 1. Field history for a one-step magnetic viscosity experiment, H_1 lying on the main loop, and a two-step magnetic viscosity experiment, H_2 lying on a minor loop (the special case leading to zero magnetization in zero field).

teron being able to exist in one of two states, i.e., bistable. The switching of hysterons between states, over an energy barrier, can be driven by the action of an applied magnetic field, as with magnetic hysteresis, or by thermal activation at a constant applied field (the latter a Preisach-Arrhenius approach⁸). A prediction of the Preisach-Arrhenius approach is the nonmonotonic behavior of the magnetic viscosity on recoil curves, with $M(t)$ first drifting in a positive direction, reaching a peak, before drifting in a negative direction. For the special case of dc demagnetization ($H_2=0$), $M(t)$, depending on the material, may drift upwards for days or months, before relaxing to zero with a time scale that may be years.

Recently, it has been reported that bulk-amorphous hard magnets can be obtained in the multicomponent alloy systems Nd-Fe-Al (Ref. 9) and Nd-Fe-Co-Al (Ref. 10). Wang *et al.*¹¹ have observed nonmonotonic behavior of the magnetic viscosity on the lower branch of minor hysteresis loops in Nd₆₀Fe₃₀Al₁₀. These materials appear to be ideal systems in which to study magnetic viscosity, in particular the nonmonotonic behavior of $M(t)$, as their magnetic properties permit observation of what is a small effect. Though they have an intrinsic coercivity of order 300 kA/m, they are unlikely to find widespread use in hard magnetic applications, due to their low remanence when compared to existing commercially available hard magnets. We have prepared bulk-amorphous Nd₆₀Fe₂₀Co₁₀Al₁₀ and performed magnetization measurements on the major hysteresis loop, and determined S , χ_{irr} , and H_f . Further measurements have been made on recoil curves (both lower and upper branches), and the special case of the recoil curve that leads to the dc demagnetized state, to investigate nonmonotonic behavior. A Preisach-Arrhenius approach is used to interpret the observed nonmonotonic behavior of the magnetic viscosity, with emphasis on exploring the relationship between the time taken for the magnetization to reach a peak and H_2 .

II. EXPERIMENT

A cylindrical sample of Nd₆₀Fe₂₀Co₁₀Al₁₀ was prepared by argon-arc melting and suction casting into a split copper mould, with a 2 mm diameter. X-ray powder diffraction studies of the sample showed it to be essentially amorphous, with only a trace (<1%) of crystallinity, which appears to be nonferromagnetic (peaks could not be indexed to the constituent elements or most probable intermetallics, e.g., NdFe₂). There is no wasting or step in the hysteresis loop (see Fig. 2), which would indicate the presence of a soft magnetic phase. The density of the Nd₆₀Fe₂₀Co₁₀Al₁₀ sample, measured by displacement, is 6.9 g/cm³. Magnetic measurements were performed at room temperature (21 °C) in applied magnetic fields (H_{app}) up to 1.5 MA/m, using a Lake Shore Vibrating Sample Magnetometer mounted on an electromagnet. All magnetic field measurements are reported in terms of the internal magnetic field H_{int} , calculated using a sample demagnetizing factor of 0.12, and magnetization measurements as the magnetic polarization J , where $J = \mu_0 M$.

The major hysteresis loop, a representative minor loop

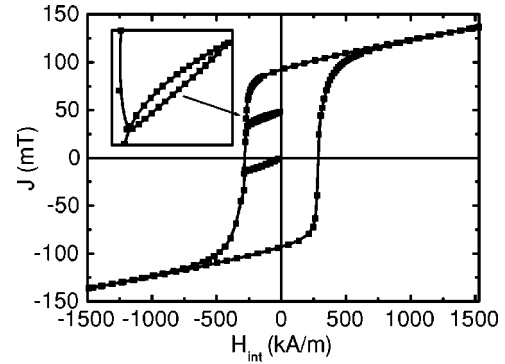


FIG. 2. Major hysteresis loop for Nd₆₀Fe₂₀Co₁₀Al₁₀, a representative minor loop, and the recoil curve that leads to the dc demagnetized state.

and the recoil curve that leads to the dc demagnetized state, are shown in Fig. 2. The behavior of the major hysteresis loop was further investigated with loops measured for a number of different sweep rates dH_{app}/dt , and these are shown, for the second quadrant, in Fig. 3. The intrinsic coercivity H_i^c , determined when $J=0$ (as the loop crosses the field axis), ranges from 325 kA/m for a sweep rate of 26 500 (A m^{-1}) sec^{-1} to 269.4 kA/m for a sweep rate of 119.4 (A m^{-1}) sec^{-1} . Over the range of sweep rates measured, H_i^c is proportional to the logarithm of the sweep rate, where $H_i^c = 290.68 + 10.2 \ln(dH_{app}/dt)$ (kA/m), where dH_{app}/dt is in units of (kA m^{-1}) sec^{-1} , with a regression coefficient of 0.999 61. This is in common with studies on nanocrystalline soft magnetic materials¹² where it has been found that the coercivity follows the expression

$$H_i^c \approx H_f \ln(dH/dt), \quad (3)$$

where H_f is an “equivalent” fluctuation field, and has, for the data shown in Fig. 3, a value of 10.2 kA/m. The strong dependence of H_i^c on sweep rate indicates a significant time-dependent magnetization. The demagnetization remanence J_{irr} was measured and the (rationalized) irreversible susceptibility κ_{irr} calculated by dJ_{irr}/dH_{int} (see Fig. 4).

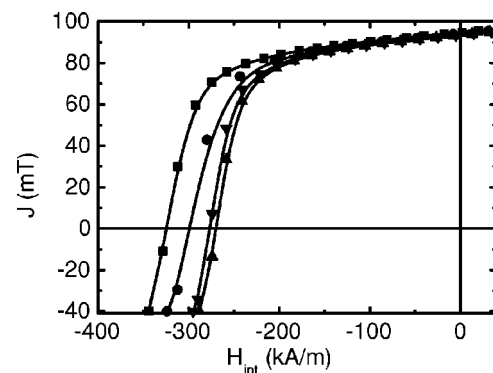


FIG. 3. Behavior of the major hysteresis loop in the second quadrant for sweep rates of (■) 26 500 (A m^{-1}) sec^{-1} , (●) 2650 (A m^{-1}) sec^{-1} , (▼) 265 (A m^{-1}) sec^{-1} , and (▲) 119.4 (A m^{-1}) sec^{-1} .

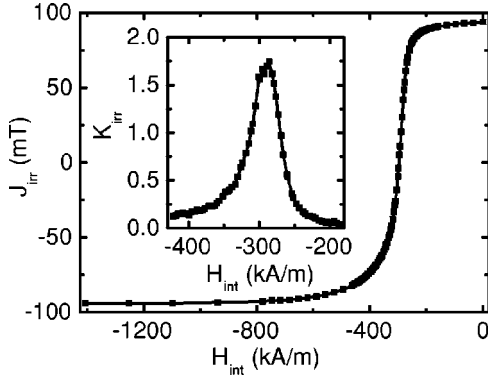


FIG. 4. Demagnetization remanence J_{irr} as a function of H_{int} and inset the (rationalized) irreversible susceptibility κ_{irr} as a function of H_{int} .

Magnetic viscosity measurements were performed for both one- and two-step processes, over time intervals up to 24 h. The following magnetic field histories were used for the measurements.

(1) For one-step processes on the main loop, the sample was first saturated in a positive applied field H_s of 1.5 MA/m. The applied field was then ramped at a rate of $795.8 \text{ (kA m}^{-1}\text{) min}^{-1}$ in a negative direction to a point on the main loop in the second or third quadrant (H_1 in Fig. 1) and held constant while the magnetization was measured as a function of time. The sequence can be summarized: $H_s = 1.5 \text{ MA/m} \Rightarrow H_1$, measure $M(t)$.

(2) For two-step processes the main focus of interest was the recoil line that leads to the dc demagnetized state. As with the one-step process, the sample was first saturated in a positive applied field H_s of 1.5 MA/m. The applied field was then ramped at a rate of $795.8 \text{ (kA m}^{-1}\text{) min}^{-1}$ in a negative direction to the turning point on the main loop, $H_1 = -290.7 \text{ kA/m}$, and paused for 6–10 sec. The field was then ramped at the same rate as before in a positive direction to a point H_2 on the recoil line (including the special case of $H_2 = 0$ and $J = 0$) and held constant while the magnetization was measured as a function of time. The sequence can be summarized: $H_s = 1.5 \text{ MA/m} \Rightarrow H_1 = -290.7 \text{ kA/m}$, 6–10 sec pause $\Rightarrow H_2$, measure $M(t)$.

(3) Two-step processes were also investigated on the lower branch of the minor loop in the second quadrant shown in Fig. 2. The procedure was identical to that used for two-step processes on the recoil curve that leads to the dc demagnetized state, with the exception that the turning point H_1 was -271.5 kA/m . The sequence can be summarized: $H_s = 1.5 \text{ MA/m} \Rightarrow H_1 = -271.5 \text{ kA/m}$, 6–10 sec pause $\Rightarrow H_2$, measure $M(t)$.

(4) The upper branch of the minor loop in the second quadrant was investigated with a more complicated field history of three steps. The procedure was identical to that used on the lower branch, with the addition that the field was ramped in a positive direction from the turning point of -271.5 kA/m to 0 kA/m and paused for 6–10 sec. The field was then ramped in a negative direction along the upper branch of the minor loop to a particular point and held constant while the magnetization was measured as a function of

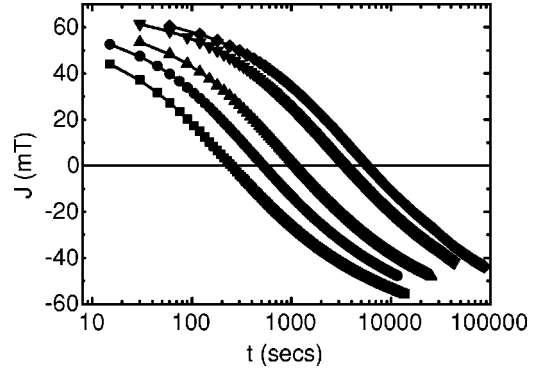


FIG. 5. Experimental results for one-step processes on the main loop showing the decay of magnetic polarization J as a function of the logarithm of time t for fixed values of applied magnetic field of (\blacklozenge) -235.6 kA/m , (\blacktriangledown) -239.6 kA/m , (\blacktriangle) -247.6 kA/m , (\bullet) -253.7 kA/m , and (\blacksquare) -259.8 kA/m .

time. The sequence can be summarized: $H_s = 1.5 \text{ MA/m} \Rightarrow H_1 = -271.5 \text{ kA/m}$, 6–10 sec pause $\Rightarrow H_{app} = 0 \text{ kA/m}$, 6–10 sec pause $\Rightarrow H_2$, measure $M(t)$.

III. RESULTS

A. Magnetic viscosity on the major loop

Experimental results for the decay of magnetic polarization for a one-step process on the main hysteresis loop for a number of fields are shown in Fig. 5. The method of Street and Brown,² based on the equation

$$\Delta H = \frac{kT}{\partial E / \partial H|_M} \ln(t) = H_f \ln(t), \quad (4)$$

is used to derive H_f . In essence, lines at fixed values of J , values ranging from -40 mT to 50 mT in increments of 10 mT , are drawn in Fig. 5. The intersection of these lines with the successive curves of the time decay of J , each at a constant field, determines ΔH and $\ln(t)$, which are plotted in Fig. 6. The gradient of these lines, as is seen from Eq. (4), gives H_f . The values of H_f obtained range from 6.5 kA/m to 7.6 kA/m , with nine out of the ten values between 7.1 kA/m and 7.6 kA/m . Excluding the value of 6.5 kA/m , the average of

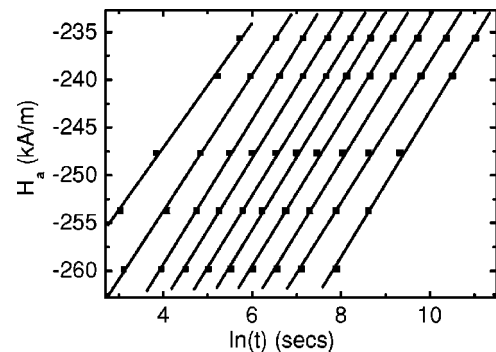


FIG. 6. H_a and $\ln(t)$ determined from the intersections of lines of constant J , from the experimental curves in Fig. 5. (Lines from left to right correspond to values of J of 50 mT , 40 mT , 30 mT , 20 mT , 10 mT , 0 mT , -10 mT , -20 mT , -30 mT , and -40 mT .)

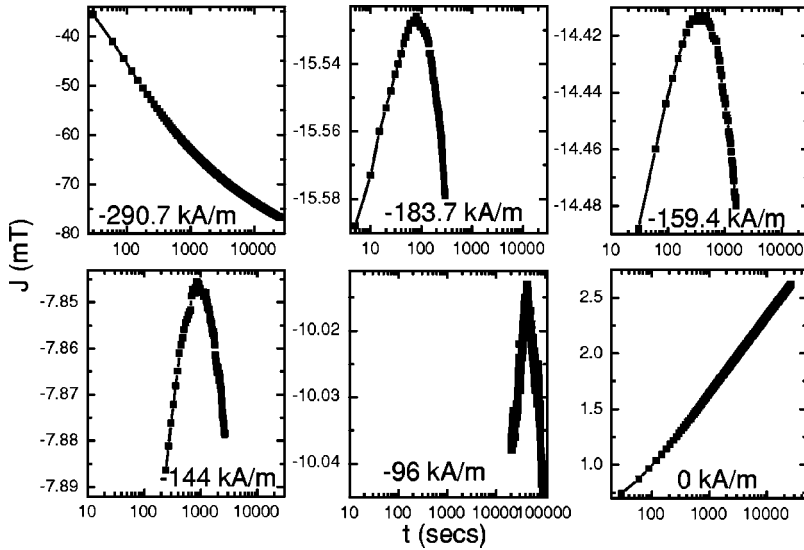


FIG. 7. Magnetic polarization J as a function of time for a number of applied fields H_2 along the recoil curve leading to the dc demagnetized state. The sequence of applied fields is from the top left to the bottom right.

the other nine values gives a value for H_f of 7.5 kA/m, which is close to the value of 9.6–10.3 kA/m reported for bulk amorphous $\text{Nd}_{60}\text{Fe}_{30}\text{Al}_{10}$.¹¹ The value for H_f of 7.5 kA/m is also consistent with the value of 10.2 kA/m obtained earlier from the approximate expression used to describe the time-dependent behavior of the coercivity.

An activation volume ν can be determined from H_f using the relationship

$$H_f = \frac{kT}{\nu M_s}, \quad (5)$$

where k is the Boltzmann constant, T the temperature, and M_s the saturation magnetization.⁵ Substituting into Eq. (5) values for T of 294 K and M_s of 111 kA/m (111 G) yields an activation volume of $4 \times 10^{-18} \text{ cm}^3$, smaller than the value of $15\text{--}20 \times 10^{-18} \text{ cm}^3$ reported for $\text{Nd}_{60}\text{Fe}_{30}\text{Al}_{10}$.¹¹ Collocott and Dunlop¹³ in a study of commercial rare-earth magnet materials report a value for the activation volume in sintered $\text{Nd}_2\text{Fe}_{14}\text{B}$ (Vacodym 400HR) of $2.6 \times 10^{-18} \text{ cm}^3$, in HDDR $\text{Nd}_2\text{Fe}_{14}\text{B}$ powder (Magnequench MQA-T) of $6.22 \times 10^{-18} \text{ cm}^3$, and in sintered $\text{Sm}_2\text{Co}_{17}$ (Vacomax 225HR) of $0.69 \times 10^{-18} \text{ cm}^3$.

The concept of the activation volume has been developed in the context of granular crystalline materials and can be viewed as the actual particle volume of a domain involved in the thermal activation process.⁵ This link to a microstructural feature is less applicable to bulk amorphous materials where there is no long-range crystalline or granular order. A feature of amorphous materials is a small activation volume; for example, values of $\approx 10^{-18} \text{ cm}^3$ are reported in TbFeCo thin films,¹⁴ similar in magnitude to the value reported here for $\text{Nd}_{60}\text{Fe}_{20}\text{Co}_{10}\text{Al}_{10}$. A related observation has been made for CrO_2 powders used in recording media, where the activation volume is much smaller than the actual particle size⁶ (particle size of order $4 \times 10^{-16} \text{ cm}^3$ compared with the activation volume of $1.5 \times 10^{-17} \text{ cm}^3$).¹⁵ This suggests that the activation volume is only weakly correlated to grain or particle size.⁶ It may be better to view the activation volume in an amorphous material as being a characteristic dimension

over which magnetic moments are correlated, forming an entity that is the basic unit for any thermally activated processes.

B. Magnetic viscosity on the recoil curve that leads to the dc demagnetized state

Experimental results for a two-step process on the recoil curve, which leads to the dc demagnetized state, are shown in Fig. 7. At the turning point $H_1 = -290.7 \text{ kA/m}$, on the main loop the magnetization is seen to decrease monotonically with time. On moving along the recoil curve—that is, moving in a positive field direction as the applied field H_2 becomes less negative—the magnetization is seen to increase initially, reaching a peak, before decreasing; that is, non-monotonic behavior is observed. The time to reach the peak, t_{max} , is dependent on H_2 and varies from a few tens of seconds at -184.2 kA/m to $\approx 12.5 \text{ h}$ at -96 kA/m .

C. Magnetic viscosity on the lower and upper branches of a minor hysteresis loop

Experimental results for a two-step process leading to the lower branch of a minor hysteresis loop, in the second quadrant, are shown in Fig. 8. The turning point H_1 is -271.5 kA/m . The behavior of magnetization is essentially identical to that observed for the recoil line leading to the dc demagnetized state. The nonmonotonic character of the magnetization as a function of time is seen clearly, and as the applied field is moved in a positive direction, the time to reach a magnetization peak increases. Again in a nominally zero field the sample remagnetizes spontaneously, with a monotonic increase in the magnetization.

The situation for a three-step process, which leads to the upper branch of the minor hysteresis loop, is somewhat different. Experimental results are shown in Fig. 9, and note that the data for the various applied fields have been plotted with the same span in J , to highlight features. In addition to the first turning point at -271.5 kA/m , there is now a second turning point at 0 kA/m , from which the field is moved

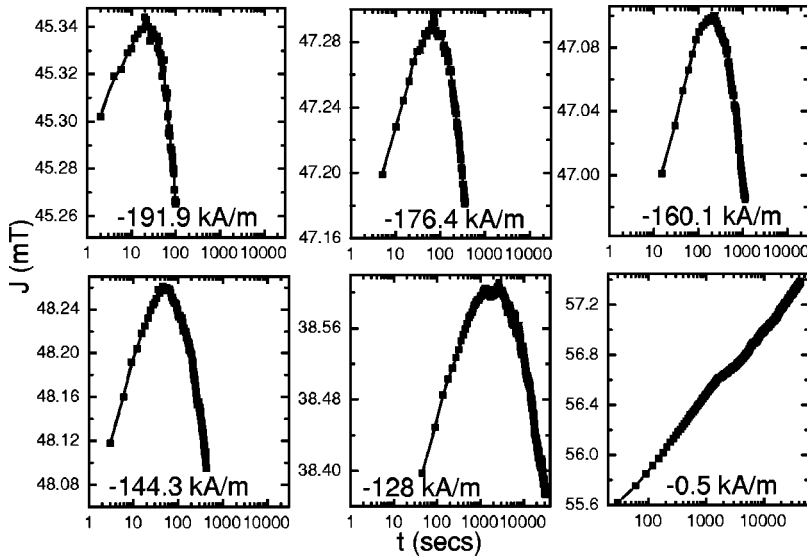


FIG. 8. Magnetic polarization J as a function of time for a number of applied fields H_2 along the lower branch of the minor hysteresis loop with $H_1 = -271.5$ kA/m. The sequence of applied fields is from the top left to the bottom right.

in a negative direction and made progressively more negative. At the two extreme points of the upper branch of the recoil curve—that is, at or near zero field and a point on the main loop—the magnetization as a function of time behaves as expected and is consistent with the observations made on the lower branch of the minor hysteresis loop and the recoil curve leading to the dc demagnetized state. Namely, at zero field there is a monotonic increase in magnetization, as the material spontaneously remagnetizes, and a monotonic decrease in the magnetization on the main loop. Along the upper branch, as the field is made progressively more negative, no clear peak is seen in the magnetization; rather the slope of the magnetization data (plotted versus the logarithm of time) is seen to become less positive, at a field of -79.1 kA/m be close to zero, as the magnetization remains constant, before becoming negative, and then increasingly negative.

IV. DISCUSSION

Nonmonotonic behavior, resulting from a two-step process, can be interpreted in the context of the Preisach model.

The key to the Preisach model is the concept that the material can be represented by a collection of hysterons. The magnetization of each hysteron is normalized being either $+1$ or -1 , depending on the value of an applied switching magnetic field. The magnetization is the sum of the contributions from the hysterons, the Preisach function is the density function of hysterons, and the up-switching field and the down switching fields are the coordinates that define the Preisach plane. It is not our intention to discuss in detail the Preisach model as this can be found elsewhere, notably the monographs of Bertotti¹ and Della Torre.⁷ Of most interest here is application of the Preisach approach to gain insight into the relationship between the time taken to reach the peak in magnetization, t_{max} , and H_2 . The nonmonotonic behavior of the magnetization from a two-step process can be described with reference to the Preisach plane, shown in Fig. 10. As the field is decreased from saturation, H_s , in a negative direction to H_1 , and then reversed, increasing in a positive direction from H_1 to H_2 where it is held constant, the two portions of the state lines, indicated by arrows, relax to

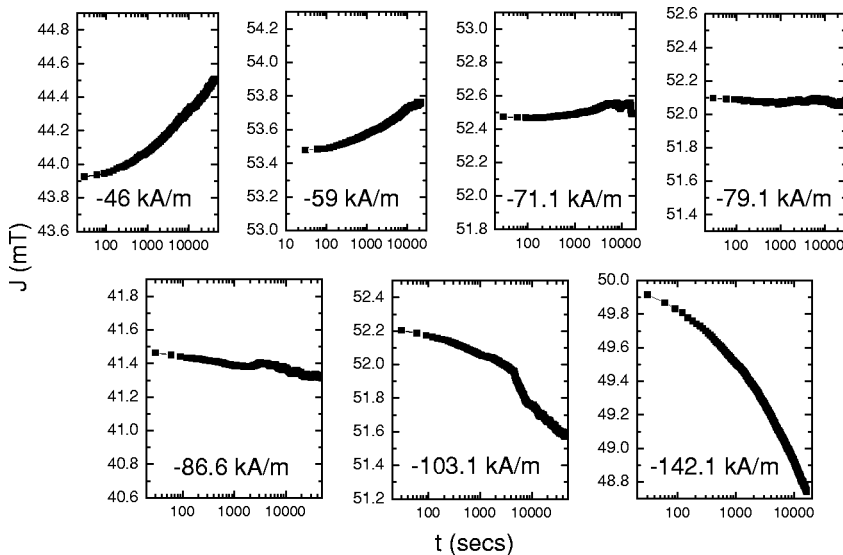


FIG. 9. Magnetic polarization J as a function of time for a number of applied fields along the upper branch of a minor hysteresis loop. The sequence of applied fields is from the top left to the bottom right.

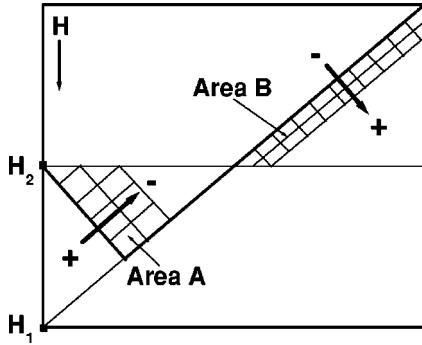


FIG. 10. The Preisach description of relaxation following a two-step field process.

give opposite contributions to the magnetization. The significant feature is that the relaxing hysterons that contribute to the magnetization in a positive manner and those hysterons which contribute to the magnetization in a negative manner have completely different time constants. This is the source of the nonmonotonic behavior of the magnetization. The magnetization first increases, as the hysterons that make up region A in Fig. 10 relax, then decreases as these hysterons are exhausted, and the relaxing hysterons in region B are the only ones contributing to the change in magnetization.

The Preisach description of the two-step process in Fig. 10 forms the basis of a simple geometrical approach, based on the relative contributions to the changing magnetization from regions A and B, to explore the relationship between t_{max} and H_2 . The approach is to derive an expression for the changing magnetization in region A, ΔM_a , and likewise for the changing magnetization in region B, ΔM_b , which contain time-dependent terms. For both regions A and B the change in magnetization is proportional to the area swept out by the state lines, but the constant of proportionality will be different for regions A and B, as the density of hysterons (i.e., the Preisach distribution) able to participate in the relaxation process falls on approaching the positive saturation field H_s . Thence the difference between ΔM_a and ΔM_b is determined ($\Delta M_a - \Delta M_b$) and differentiated with respect to time and equated to zero to determine the behavior of t_{max} . It is assumed that the state lines move at two different constant logarithmic rates and in each case traverse equal numbers of hysterons per unit distance. Under such circumstances the magnetization would display a simple logarithmic time dependence in a single-step experiment. This is the case for our sample in the region of interest, as the magnetization data shown in Fig. 5 display this characteristic. From the discussion in Bertotti¹ (see pp. 500–503), for region A, the relaxation rate τ_A and the distance traversed by the state line, h_A , are given by (for $t \gg \tau_0$, with τ_0 viewed as a time interval over which the system updates its state)

$$\tau_A = \tau_0, \quad (6)$$

$$h_A = C \ln\left(\frac{t}{\tau_0}\right), \quad (7)$$

and for region B, the relaxation rate τ_B and the distance traversed by the state line, h_B , by

$$\tau_B = \tau_0 \exp\left(\frac{\Delta H}{H_f}\right), \quad (8)$$

$$h_B = C \ln\left(\frac{t}{\tau_0}\right) - C \left(\frac{\Delta H}{H_f}\right), \quad (9)$$

where C is a constant and $\Delta H = (H_2 - H_1)$.

The contribution to the magnetization arising from relaxation in region B will be of the form

$$\Delta M_B = C_B h_B, \quad (10)$$

where C_B is a constant. The time-dependent component of ΔM_B is

$$\Delta M_B(t) = C_B C \ln(t). \quad (11)$$

For region A, it is first necessary to evaluate the crosshatched area, which equals

$$\frac{1}{4}[(\Delta H)^2 - (\Delta H - h_A)^2] = \frac{1}{4}(2h_A \Delta H - h_A^2) \quad (12)$$

and the time-dependent terms in ΔM_A ,

$$\Delta M_A(t) = \frac{C_A C}{4} [2\Delta H \ln(t) - C(\ln(t))^2 + 2C \ln(t) \ln(\tau_0)], \quad (13)$$

where C_A is a constant. The maximum (peak) in the magnetization will occur at a time t_{max} , where

$$\begin{aligned} \frac{\partial[\Delta M_A(t) - \Delta M_B(t)]}{\partial t} &= \frac{C_A C}{4t_{max}} [2\Delta H - 2C \ln(t_{max}) \\ &\quad + 2C \ln(\tau_0)] - \frac{C_B C}{t_{max}} \\ &= 0 \end{aligned} \quad (14)$$

and therefore

$$C_A[\Delta H - C \ln(t_{max}) + C \ln(\tau_0)] - 4C_B C = 0, \quad (15)$$

which, after simplifying and ignoring the terms that are constant along a particular minor loop, gives

$$\ln(t_{max}) \propto H_2. \quad (16)$$

For different minor loops, C_B will change, and therefore plots of $\ln(t_{max})$ versus H_2 will have the same slope but different intercepts.

This simple geometric approach predicts the functional relationship between the time at which the peak in the magnetization occurs and H_2 . The data for t_{max} and H_2 are plotted in Fig. 11 for both the recoil line leading to the dc demagnetized state, $H_1 = -290.7$ kA/m, and for the lower branch of the minor hysteresis loop, $H_1 = -271.5$ kA/m. It is seen that the approach adopted is general to both sets of data and provides a reasonable approximation for the functional relationship between t_{max} and H_2 . Both the curves

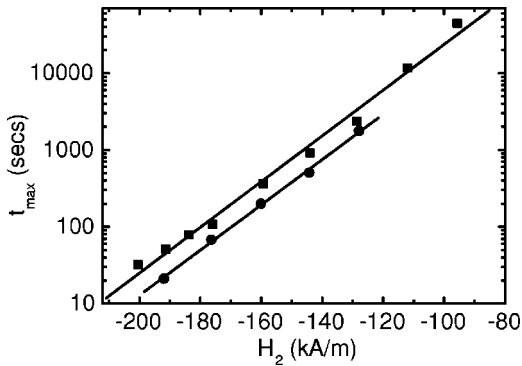


FIG. 11. The time t_{max} at which the peak in the magnetization occurs as a function of H_2 . The upper curve is for data on the recoil line leading to the dc demagnetized state, $H_1 = -290.7$ kA/m, and the lower curve for data on the lower branch of the minor hysteresis loop with $H_1 = -271.5$ kA/m.

plotted in Fig. 11 have the same slope but there is a small offset in the y intercept, as C_B is different for data obtained for different minor loops.

Nonmonotonic behavior of the magnetization is a universal feature of a two-step process in ferromagnetic materials, its observation being dependent on key material properties and experimental conditions. The effect may occur over very short time scales or very long time scales, even years, or there may be very small changes in the magnetization making its experimental observation impractical. The key to the observation of the effect in the Preisach description is the relaxation rate for area B, given by Eq. (8), and in particular the behavior, and sensitivity, of this function with respect to the values of H_1 and H_f . With reference to the data for the recoil line leading to the demagnetized state, $H_1 = -290$ kA/m, $H_f = 7.5$ kA/m, and $\tau_0 \approx 10^{-10}$ sec (based on the estimates given in Refs. 1 and 16), it can be seen that τ_B varies from 1.62×10^{-4} sec for $H_2 = -183.7$ kA/m to 18 sec for $H_2 = -96$ kA/m. For the latter, nonmonotonic behavior is observable over a time scale of 28 h. For the special case of $H_2 = 0$ kA/m, $\tau_B = 6.8 \times 10^6$ sec and the magnetization is

seen to be still increasing after 24 h, and it would be necessary to wait of the order of 1 year before a peak is observed followed by a subsequent decrease in the magnetization. (This is a somewhat impractical experiment.) The effect of H_2 , as it becomes more negative, is to give values of τ_B that enable observation of nonmonotonic behavior over readily accessible experimental time scales. H_f is a property of the material, but for materials that have a small value, such as hard magnets, e.g., Alnico,⁵ $H_f \approx 80$ A/m, and NdFeB,¹³ $H_f \approx 1$ kA/m, the term $(\Delta H/H_f)$ gets larger more quickly, as does τ_B , making observation of nonmonotonic behavior difficult, as the range of field values H_2 is limited and time scales are increasingly short. In the limit as H_f gets very small, the difference $(H_2 - H_1)$ must also become small if nonmonotonic behavior is to be observed, but a point may be reached where experimentally it is impractical due to limitations on magnet sweep rates and the inability to make field changes in small increments. It is desirable to have a material with $H_f \approx 8$ kA/m, as is the case in bulk-amorphous ferromagnets, making these materials ideal for studying nonmonotonic behavior. For the experimental conditions used in this work, $(\Delta H/H_f)$ has to be in the range $\approx 14-25$, for observation of nonmonotonic behavior.

V. CONCLUSION

Nonmonotonic behavior in the magnetization has been observed in the bulk-amorphous ferromagnet $\text{Nd}_{60}\text{Fe}_{20}\text{Co}_{10}\text{Al}_{10}$. The Preisach model has been used to interpret this nonmonotonic behavior and shows $\ln(t_{max}) \propto H_2$. It is argued that nonmonotonic behavior is a universal feature of a two-step process in ferromagnetic materials, its observation being dependent on key material properties and experimental conditions. The time scale of the evolution of the peak in the magnetization may make its experimental observation impractical. In general a material with a fluctuation field of order 8 kA/m is desirable if nonmonotonic behavior is to be observed with ease.

*Corresponding author. Electronic address: stephen.collocott@csiro.au

¹Giorgio Bertotti, *Hysteresis in Magnetism for Physicists, Materials Scientists and Engineers* (Academic Press, San Diego, 1998).

²R. Street and S.D. Brown, *J. Appl. Phys.* **76**, 6386 (1994).

³R. Street and J.C. Woolley, *Proc. R. Soc. London, Ser. A* **62**, 562 (1949).

⁴K.-H. Müller *et al.*, in *Proceedings of the 9th International Symposium on Magnetic Anisotropy and Coercivity in Rare-Earth Transition Metal Alloys, Sao Paulo, 1996*, edited by F. P. Missell, V. Villas-Boas, H. R. Rechenberg, and F. J. G. Landgraf (World Scientific, Singapore, 1996), p. 381.

⁵E.P. Wohlfarth, *J. Phys. F: Met. Phys.* **14**, L155 (1984).

⁶A. Lyberatos and R.W. Chantrell, *J. Phys.: Condens. Matter* **9**, 2623 (1997).

⁷Edward Della Torre, *Magnetic Hysteresis* (IEEE Press, Piscata-

way, NJ, 1999).

⁸E. Della-Torre, L.H. Bennet, and L.J. Swartzendruber, *Mater. Res. Soc. Symp. Proc.* **517**, 291 (1998).

⁹A. Inoue, A. Takeuchi, and T. Zhang, *Metall. Mater. Trans. A* **29**, 1779 (1998).

¹⁰G.J. Fan, W. Loser, S. Roth, J. Eckert, and L. Schultz, *J. Mater. Res.* **15**, 1556 (2000).

¹¹L. Wang, J. Ding, Y. Li, Y.P. Feng, and X.Z. Wang, *J. Magn. Magn. Mater.* **206**, 127 (1999).

¹²V. Basso, M. LoBue, C. Beatrice, P. Tiberto, and G. Bertotti, *IEEE Trans. Magn.* **34**, 1177 (1998).

¹³S.J. Collocott and J.B. Dunlop, *J. Phys. D* **30**, 1477 (1997).

¹⁴A. Chekanov, K. Matsumoto, and K. Ozaki, *J. Appl. Phys.* **90**, 4657 (2001).

¹⁵L. Folks and R. Street, *J. Appl. Phys.* **76**, 6391 (1994).

¹⁶M. LoBue, V. Basso, G. Bertotti, and K.-H. Müller, *IEEE Trans. Magn.* **33**, 3862 (1997).